The Effect of Force Saturation on the Haptic Perception of Detail

Marcia O'Malley, *Associate Member, IEEE,* and Michael Goldfarb, *Member, IEEE*

***Abstract*—This paper presents a quantitative study of the effects of maximum capable force magnitude of a haptic interface on the haptic perception of detail. Specifically, the haptic perception of detail is characterized by identification, detection, and discrimination of round and square cross-section ridges, in addition to corner detection tests. Test results indicate that performance, measured as a percent correct score in the perception experiments, improves in a nonlinear fashion as the maximum allowable level of force in the simulation increases. Further, all test subjects appeared to reach a limit in their perception capabilities at maximum-force output levels of 3–4 N, while the hardware was capable of 10 N of maximum continuous force output. These results indicate that haptic interface hardware may be able to convey sufficient perceptual information to the user with relatively low levels of force feedback. The data is compiled to aid those who wish to design a stylus-type haptic interface to meet certain requirements for the display of physical detail within a haptic simulation.**

***Index Terms*—Design specifications, haptic interface, haptic perception, virtual environment.**

I. Introduction

THE PROPER design of any machine requires a well-defined set of design specifications. Hardware design specifications for haptic interfaces that relate machine parameters to human perceptual performance are notably absent in the literature, although much work has been accomplished in the field in general (see, for example, the surveys [1], [2]). The absence of these specifications is due primarily because haptic interface design specifications must consider issues of human perception. Human perception, in turn, is complex in nature and difficult to assess quantitatively.

With the recent introduction of several commercially oriented haptic devices and applications, the need for a set of design specifications to guide the cost-optimal design of haptic devices is that much more pronounced. The work presented in this paper is an attempt to characterize the effects of one haptic interface design specification, maximum endpoint force, on the ability of a human to haptically perceive and distinguish the haptic display of detail. Along with similar characterizations of other design specifications, this work should help form a set of design specifications from which a designer can properly and perhaps more effectively design a stylus-type haptic interface for a given application.

One prior attempt to elucidate the relationship between haptic device design and human perception was the work of MacLean, who investigated the effects of machine sampling frequency and mechanical damping on human perception, and suggested "preliminary" design guidelines for these traits [3]. She further suggested the existence of a disparity between machine quality and function, which is a notion that is corroborated by the findings of this paper.

Despite this effort, the vast majority of the research literature related to this topic has generally either focused on quantitative measures of human factors, measures of machine performance independent of human perception, or the effects of software on haptic perception of virtual environments. Regarding the first area, psychophysical experiments conducted by several research groups have quantified several haptic perception characteristics, such as pressure perception, position resolution, stiffness, force output range, and force output resolution (see, for example, [4]–[8]). Since these experiments did not involve haptic interface equipment, however, they were not able to create a direct link between machine performance and human perception during haptic task performance. The experiments performed on length resolution by Durlach *et al.* [8], for example, quantified the limits (i.e., size identification and discrimination) of human perception of actual objects, but did not draw parallels between human perceptual ability and haptic hardware design.

Within the second area of research, optimal machine performance has been characterized in the literature, yet these measures are typically disparate from human perceptual measures. When designing high-performance equipment, designers seek to build a device with characteristics such as high-force bandwidth, high-force dynamic range, and low apparent mass [9], [10]. These are typically qualitative specifications, however, since the designers have little reference information regarding the quantitative effects of these machine parameters on the performance of humans with regards to perception in a haptically simulated environment. While designers are aware of the benefits of "high" bandwidth and "high"-force dynamic range, there is a lack of quantitative data to illustrate the relationship between these design parameters for a haptic device and human perception. Several researchers have incorporated human sensory and motor capability as a prescription for design specifications of a haptic interface [11], [12]. Such measures are logical, though indirectly related to haptic perception and most likely quite conservative for common haptic tasks. Colgate and Brown offer qualitative suggestions for haptic machine design

Manuscript received August 23, 2000; revised May 16, 2001. This work was supported by the National Aeronautics and Space Administration (NASA) under Grant NGT-8-52859. Recommended by Technical Editor M. Meng.

M. O'Malley was with the Department of Mechanical Engineering, Vanderbilt University, Nashville, TN 37235 USA. She is now with the Department of Mechanical Engineering and Materials Science, Rice University, Houston, TX 77005 USA (e-mail: omalleym@rice.edu).

M. Goldfarb is with the Department of Mechanical Engineering, Vanderbilt University, Nashville, TN 37235 USA (e-mail: goldfarb@vuse.vanderbilt.edu).

Publisher Item Identifier 10.1109/TMECH.2002.802725.

Fig. 1. Test subject seated at haptic interface holding stylus with dominant hand. Insert shows close-up of stylus and recommended handgrip.

that are conducive to the stable simulation of high impedances [13]. Though simulation of a high impedance is a logical performance objective for a haptic device, the objective is not directly based upon measurements of human perception.

Finally, researchers have studied the effects of software on the haptic perception of virtual environments (see, for example, [14]–[16]). Morgenbesser *et al.*, for example, looked at the effects of force shading algorithms on the perception of shapes [16]. Again, these experiments did not address the relationships between haptic interface hardware design and haptic perception.

The purpose of the work presented in this paper is to fill the void in establishing a set of quantitative relationships between machine performance and haptic perception. Specifically, this paper presents quantitative data on the effects of force saturation (i.e., maximum capable endpoint force) on the haptic display of detail in a stylus-type haptic device.

II. Methods

Three psychophysical concepts are generally used to quantify perception, namely detection, discrimination, and identification. Detection experiments, used to determine absolute detection thresholds, disclose the smallest parameter value that a subject can perceive. For example, circles of varying diameter could be displayed one at a time on a screen in front of a subject. Detection experiments would be used to determine the smallest diameter circle that the subject can see. Unlike detection experiments, discrimination experiments reveal differential thresholds, or more specifically, the smallest perceivable difference in a parameter between a reference and a test object [17]. For example, discrimination experiments would show sets of two circles side by side to determine the smallest size difference between two circles that the subject could discern. Finally, absolute identification paradigms measure a person's ability to categorize parameter values without providing explicit references. An identification experiment might be used to determine how many sizes of circles in a given diameter range could be correctly classified by a subject who is shown one circle at a time. Collectively, when applied to haptic perception, these three perceptual measures serve to characterize the haptic display of detail.

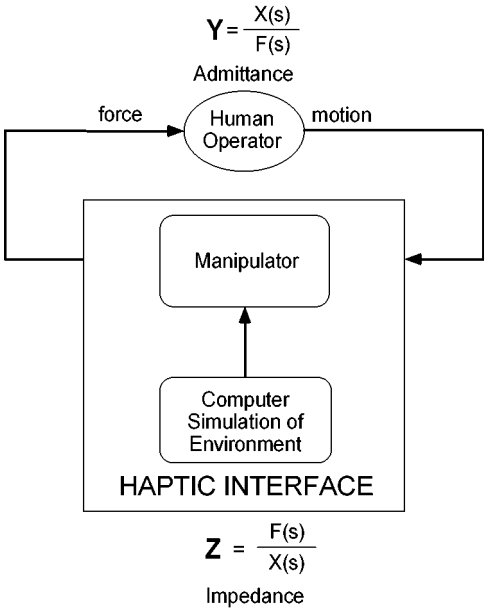

Fig. 2. Block diagram of the operator-interface feedback loop.

A. Apparatus

A three degree-of-freedom manipulator, shown in Fig. 1, was designed to exhibit low rotational inertia, minimal friction forces, zero backlash, and high-link stiffness [18], which are physical characteristics generally known to facilitate high-fidelity haptic simulations [9]. The manipulator is a point-contact force-reflecting device that interfaces with a human through a pencil-type stylus device. Together with computer software designed to simulate virtual environments, the manipulator was used to run a battery of experiments to test the effects of machine design on human perception through a haptic interface.

In the experiments described, the manipulator and haptic simulation were utilized as an impedance operator, as illustrated in Fig. 2. The haptic interface, therefore, measured 3-D motion and displayed the appropriate 3-D force vector, while the human operator was assumed to perform the inverse (admittance) operation. All simulations ran at a sampling frequency of 3000 Hz. System bandwidth is approximately 100 Hz, limited by first-order low-pass filters placed on each of the motor torque command signals. This particular apparatus is capable of displaying constant forces of over 10 N in the spatial region of the haptically displayed ridges, and peak forces of roughly 40 N.

B. Experimental Paradigms

Perception experiments were conducted for ridges of square and hemicylindrical cross-sections, since both shapes can be characterized with a single parameter, namely the diameter (or radius) for the rounded ridges and the edge length for square ridges. These two shapes were chosen because of the similarities in their cross-sectional area for ridges of the same base width. Additionally, any differences between sharp-edged and smooth features would presumably appear in test results. These basic geometries can be easily combined to form more complex geometries. Fig. 3 shows a 3-D representation of a hemicylindrical ridge (i.e., semicircular cross section).

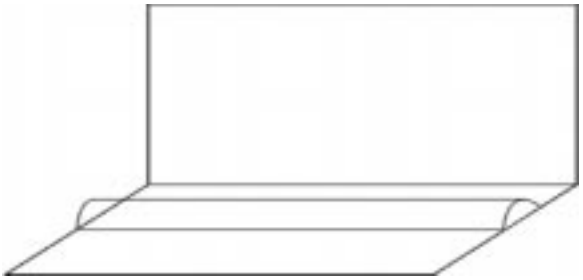

Fig. 3. Representation of a haptically rendered ridge with round cross section.

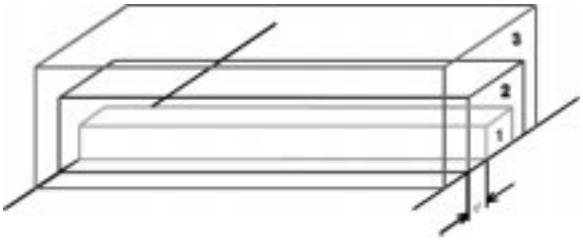

Fig. 4. Representation of square cross-section ridges in three rendered sizes showing ridge size difference, d.

The complete set of experiments consists of seven sets of data. These are size identification of square and round cross-section ridges (experiments 1A and 1B), detection of square and round cross-section ridges (experiments 2A and 2B), corner detection (experiment 3), and size discrimination of square and round cross-section ridges (experiments 4A and 4B).

During the training sessions and experiments, each subject sat in front of the haptic interface with the dominant hand holding the stylus and the nondominant hand typing responses on a keyboard. There were no measures taken to obstruct the subject's views of the haptic interface during testing. Since the objective of this work is to explore only the effects of machine parameters on haptic perception, no synthetically generated visual or audio feedback was included in the simulation. Subjects reported that the tasks relied heavily on their sense of touch and little on their sense of sight, despite the ability to see the motion of their hands.

C. Subjects

Six test subjects were used for each experiment. These subjects were chosen from a pool of individuals with varying amounts of experience using a haptic interface. A cross section of subject types (gender, dominant handedness, and experience with haptic devices) was chosen for each of these experiments.

D. Procedures

1) Experiment 1—Size Identification: Size identification tasks determine the ability of a test subject to classify similarly shaped objects, presented one at a time, by size alone. The objects in this case were synthetic ridges displayed on a virtual floor. The center of each ridge was located along the same line in the manipulator's workspace. Additionally, the floor of the simulated environment was always along the same plane. Each ridge extended across the entire workspace of the manipulator such that if the subject slid the probe along the virtual floor from the front of the workspace to the rear of the workspace in any direction, they would intersect the synthetic ridge. Both semicircular and square cross-section ridges were used in testing. All surfaces were represented as a spring and one-way damper with a spring stiffness of 1100 N/m. The damping ratios utilized were 100 Ns/m for square and 10 Ns/m for round objects, each selected for best overall simulation quality, as determined by the first author.

For experiment 1, each subject was presented with six sessions of testing. A single session consisted of one set of ridge sizes and several randomly presented levels of maximum-force feedback. For each of the six sessions, the smallest ridge size remained constant, with a radius of 10 mm for the round objects (diameter of 20 mm), and an edge length of 20 mm for the square objects. The medium and large ridges for each set of sizes were simulated by adding a constant to the radius of the small round ridge and adding twice the constant to the edge length of the small square ridge. In both cases, this constant is referred to as the variable d, or the ridge size difference. Tan found that the same information could be gathered from experiments testing identification of three distinct sizes as could from those testing four or eight sizes [19]. Therefore, to limit the number of trials necessary for experimentation, three distinct sizes of ridges were used in all size identification experiments. Fig. 4 illustrates the three sizes for square cross-section ridges.

TABLE I
RIDGE SIZES FOR EACH TESTING SESSION

Session Number	Force Saturation Values (N)	d, Size Difference (mm)	Number of trials
1	5, 10	1.25	90
2	0.75, 1.25,3, 5, 10	2.50	225
3	0.5, 0.75, 1.25, 3, 5, 10	5.00	270
4	0.5, 0.75, 1.25, 3, 5, 10	7.50	270
5	0.5, 0.75, 1.25, 3	10.00	180
6	0.5, 0.75	12.50	90

Preliminary experimentation using the first author as a test subject was performed to determine the range of object sizes to use in each session of experiment 1. The synthetic ridges displayed in these preliminary tests were implemented with full force feedback (i.e., no force saturation). The set of three ridge sizes with the smallest d value that was consistently and correctly identified by the author was used as the set with the greatest d value in final experimentation. Smaller d values would be more difficult to identify by size and would presumably generate percent correct values less than 100%. Table I outlines the ridge sizes used for each testing session.

Generally, a minimum of $5k^2$ number of trials is sufficient for identification task testing purposes, where k is the number of categories into which items can be categorized [19], [20]. In this case, since three ridge sizes were presented in each session, a minimum of 45 ridges (where $k = 3$) was necessary for each test point, where a test point consisted of one value of d and one value of maximum-force feedback level. In this experiment, since each session corresponded to one value for d, it was necessary to present 45 times the number of force feedback levels used in a particular session to the test subject.

A training session occurred before each testing session, allowing the test subject to learn the three ridge sizes for that

particular session. During the training period, subjects were presented with a virtual ridge displayed without force saturation and were then prompted to enter the number corresponding to that size on a computer keyboard. The subjects classified the ridges by entering a 1 (smallest size), 2 (medium size), or 3 (largest size) on the keyboard. If correct, the user heard a beep and went directly to a new bump. If incorrect, the size number of the simulated object was displayed on the computer monitor for the subject to see. After hitting ⟨Enter⟩, the next ridge would be displayed. The test subject was allowed to continue training for as long as s/he felt necessary. Instructions indicated that training should cease when the subject felt comfortable with the sizes and confident that s/he could classify ridges by size to the best of their ability. Most test subjects used 20–50 trials in the training sessions, depending on the difficulty of the session. The level of force feedback in the training sessions was not altered so that test subjects were trained with the highest simulation quality possible for this hardware.

During experimentation, the level of maximum-force feedback was controlled by a saturation imposed by the computer code. A single test session randomly presented objects of three sizes and between two and six levels of maximum-force feedback. As a result, ridges in the same session could feel soft or hard, depending on the maximum level of force feedback for that particular trial. The subjects were instructed to classify the randomly presented ridges into one of the three size categories for that particular trial.

2) Experiments 2 and 3—Object and Corner Detection: Object detection tests determined the smallest detectable ridge sizes in the simulated environment, while corner detection tests determined the smallest ridge sizes on which the subject could detect sharp corners. For tests of object detection and corner detection for varying levels of force feedback saturation, ridges of either square or round cross section were presented at random positions between a simulated stiff front wall and a simulated stiff back wall approximately 10 cm apart. Object locations were limited only so that the entire ridge would be displayed on the floor between the walls with no intersection. The same surface representation was used, with all spring stiffnesses equal to 1100 N/m and all damping ratios equal to 10 Ns/m for consistency of simulation feel. Subjects were asked to reply "n" for no ridge present, "s" for square ridge (object with sharp corners), and "r" for round ridge (object with no sharp corners). Ridge sizes were varied from a radius of zero to 5.0 mm for these tests. For square ridges, the radius refers to half of the edge length.

Three test sessions were performed, and subjects were allowed to practice the experiment with correct-answer feedback in a saturation-free session prior to testing. The first two sessions used identical test points, with four presentations of each combination of (ridge size)–(shape)–(force saturation level). The values of ridge sizes were an approximate logarithmic distribution over a range that included radii of 0 mm (no ridge present), radii less than 1 mm (objects are detectable but corners are difficult to perceive) to radii greater than 1 mm (objects are easily detectable and corners are perceivable). Six sizes were tested (0, 0.2, 0.4, 0.8, 2.0, and 5.0 mm) at six force saturation levels (0.5, 0.75, 1.25, 3.0, 5.0, and 10.0 N) for a total of 288 trials per experiment. These force saturation levels were the same used in all perception experiments described in this paper and are approximately distributed logarithmically across the continuous force output range of the haptic interface hardware used in experimentation. A third session was administered for the collection of data at two additional ridge sizes. This test used four ridge sizes (0, 0.1, 0.15, and 0.8 mm) and the same six levels of force saturation with four presentations of each (ridge size)–(shape)–(force saturation level) combination. The occurrence of sizes 0.1 and 0.15 mm was doubled in order to collect all data for these sizes in one session. The inclusion of sizes 0 and 0.8 mm was selected so that "n" was a valid response for this experiment, and so that one of the ridge sizes was easily detectable for high-force saturation levels. This session also presented 288 trials to the subject.

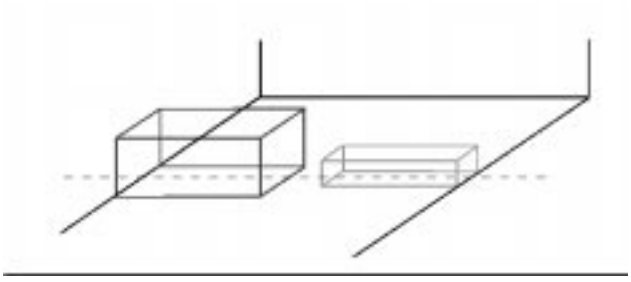

Fig. 5. Square-ridge size discrimination environment showing centerline of each ridge along the same line.

3) Experiment 4: Size Discrimination: The final experiment for the evaluation of force saturation on haptic perception was size discrimination. These discrimination experiments test the ability of a human subject to notice size differences between objects placed side by side. For this set of tests, square and round ridges were presented in separate groups. For either test, ridges were displayed side-by-side along a common centerline in the haptic interface workspace, as shown in Fig. 5. Except for a space of 2 cm between the objects, the outside edges extended to the limits of the workspace. All surfaces were represented as a spring and one-way damper with parameters as previously described.

For each session, a random selection of "left" or "right" was made within the simulation code, and the ridge corresponding to this position was defined to have a radius of 1.0 cm. To set the discrimination size d, one of six sizes was selected at random and added to a radius of 1.0 cm. This became the size of the other ridge in the simulation. The subject was asked to feel the exterior of the two ridges and determine which was larger, entering a response of "l" for left, "r" for right, or "n" for neither ridge. Six ridge discrimination sizes were used (0, 1.25, 2.50, 5.00, 7.50, and 10.00 mm) with six force saturation levels (0.5, 0.75, 1.25, 3.0, 5.0, and 10.0 N). Seven presentations of each combination comprised one session, for a total of 252 trials per session. Two complete sessions were conducted for each test subject. Again, a training session was allowed prior to each test session that mimicked the actual experiment, yet gave feedback after each user response and did not include force saturation. Test subjects were allowed to determine the amount of training they underwent.

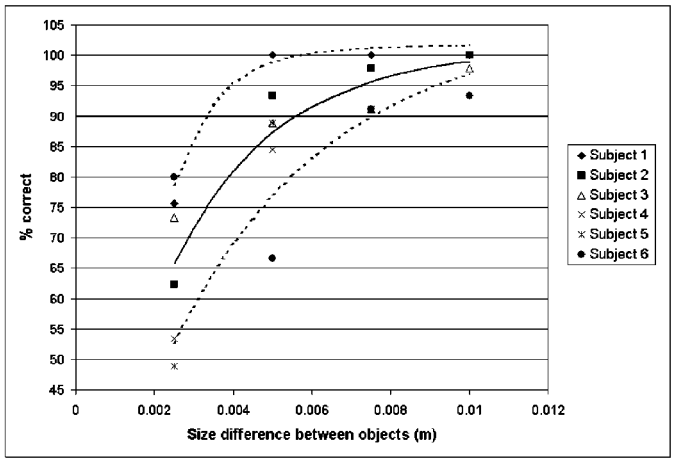

Fig. 6. Representative data for experiment 1A (square-ridge size identification) for all subjects. maximum-force output level is 3 N. Percent correct score for all subjects are shown, including average and standard deviation curve fits.

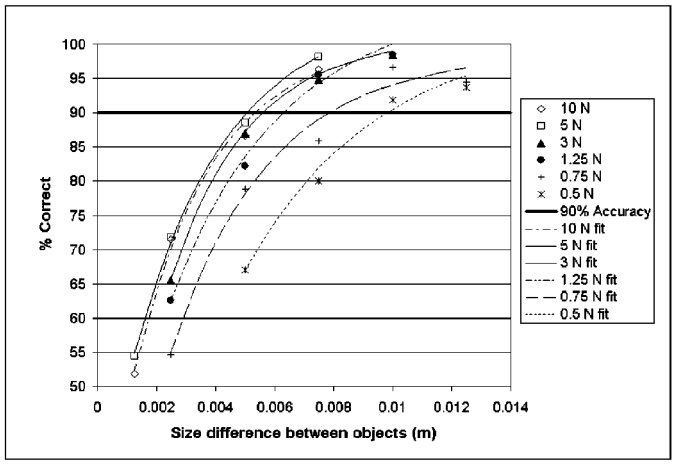

Fig. 7. Summary plot of experiment 1A results (square-ridge size identification) for all maximum-force feedback levels.

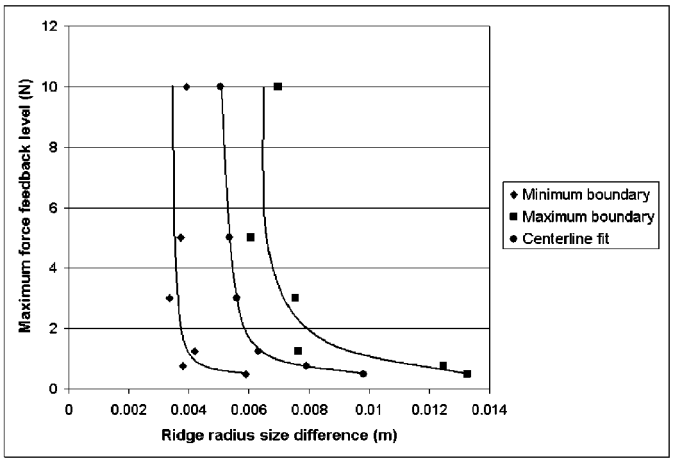

Fig. 8. Maximum force versus ridge "radius" size difference (d) for experiment 1A (square-ridge size identification).

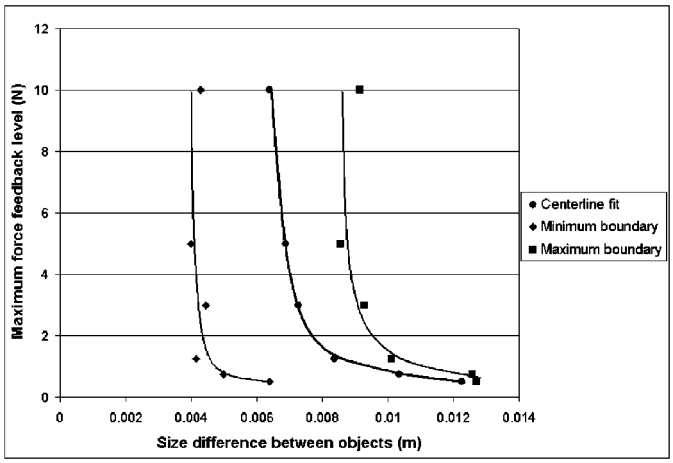

Fig. 9. Maximum force versus ridge radius size difference (d) for experiment 1B (round cross-section size identification).

III. Results

A. Experiment 1

Experiment 1 studied the ability of subjects to classify objects presented one at a time by size. Square-ridge testing was conducted in experiment 1A, while round ridge testing was conducted in experiment 1B.

The percent correct scores for each test subject were plotted versus feature size difference for each maximum-force level. Each data point shown in Fig. 6 corresponds to the averaged data for one subject, which represents the percent correct score across 45 trials. The results were then averaged across all test subjects, and a least squares curve fit was performed, utilizing an equation of the form

$$y = C_1 e^{-\lambda_1 x} + C_2 e^{-\lambda_2 x} \tag{1}$$

where C_1, λ_1, C_2, and λ_2 were curve-fitting parameters. Note that a two-component exponential curve was utilized because it yielded a noticeably better fit than did a simple exponential. In the figure, the solid line represents this exponential curve fit to the average data across all subjects. The dotted lines show the exponential curve fits to the average plus and minus one standard deviation across all subjects. Note that, as expected, the standard deviation becomes smaller as the ridge size difference increases. The data in Fig. 6 correspond to one level of maximum endpoint force, and are representative of that for all other maximum-force levels.

The exponential curves corresponding to average percent correct scores for all subjects were plotted versus each ridge size difference set for all force saturation levels. The results for experiment 1A are pictured in Fig. 7. Standard deviation curves are not shown in the figure. A 90% correct line was added to the graph to show what the authors regarded as a good level of correct size identification. The point where each exponential curve fit crossed this 90% correct line was calculated from the curve fit equations, and the resulting data pairs were plotted in Fig. 8. The graph shows maximum-force feedback levels versus difference in ridge radius for experiment 1A. A trend line is overlaid to illustrate this relationship. In addition to the data for the average among test subjects, standard deviations are also plotted. To generate these values, the average values plus and minus one standard deviation, used to create the dotted bands shown in Fig. 6, were plotted on the percent correct–ridge size difference

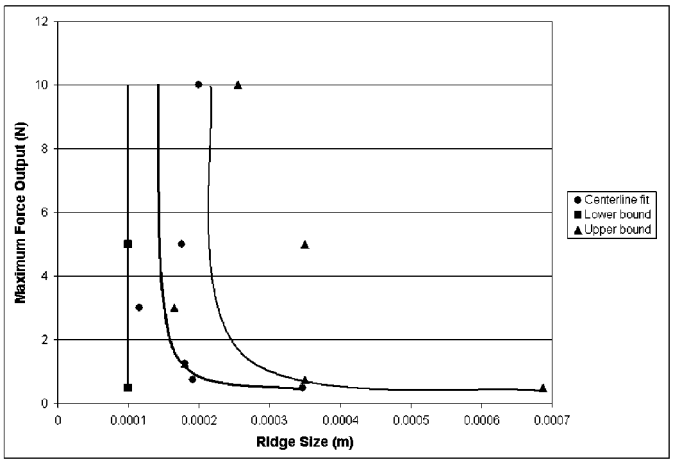

Fig. 10. Experiment 2A (square-ridge detection) summary. Maximum-force output versus ridge size for 90% accuracy.

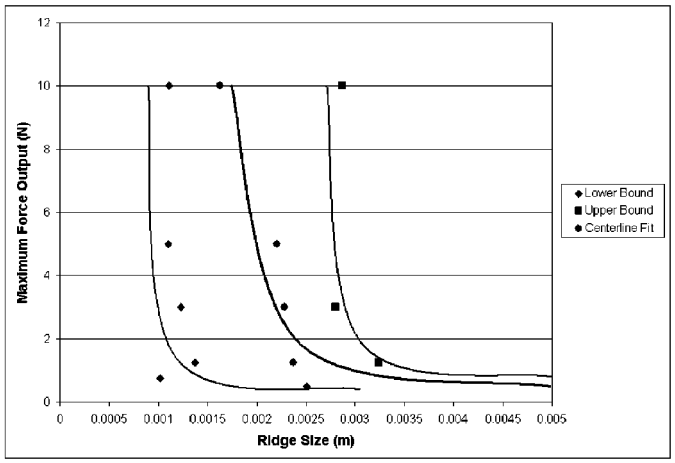

Fig. 12. Experiment 3 (corner detection) summary. Maximum-force output versus ridge size for 90% accuracy.

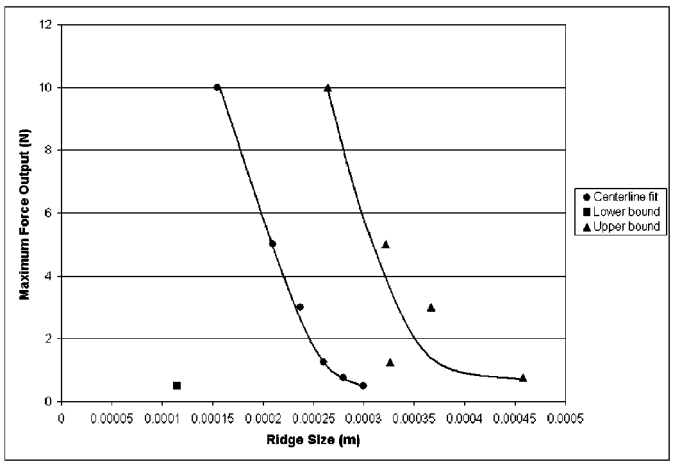

Fig. 11. Experiment 2B (round ridge detection) summary. Maximum-force output versus ridge size for 90% accuracy.

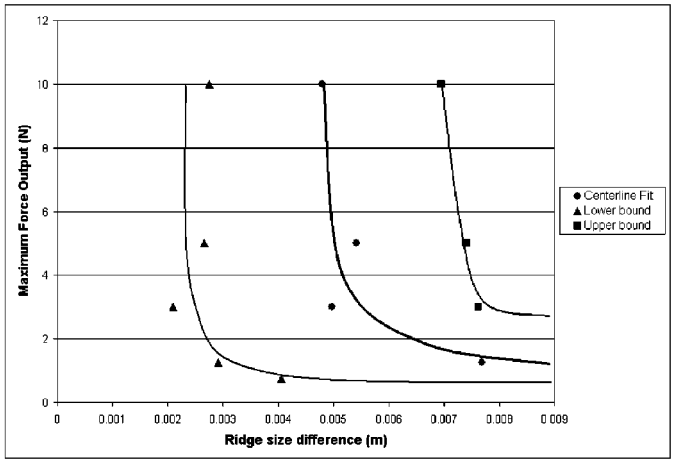

Fig. 13. Experiment 4A (square-ridge size discrimination) summary. Maximum-force output versus ridge size difference for 90% accuracy.

axes. Exponential curve fits using the two-component equation given previously were performed on the plus/minus standard deviation curves and the 90% correct crossover points were evaluated and plotted on the graph in Fig. 8.

The same procedures were followed when recording and compiling data for the size identification tasks involving objects with semicircular cross-sections. The summary experiment 1B results, generated in the same manner as that described for experiment 1A, are shown in Fig. 9.

B. Experiment 2

Percent correct scores for the detection of square (experiment 2A) and round (experiment 2B) features were examined. Data collected during testing were of the same form as the size identification results. Percent correct scores were tallied verses the size of the objects to be detected. In these graphs, size refers to radius of round ridges, or half of edge length for square ridges. Summary graphs of results were prepared using the same methods as described for size identification. Results for all test subjects for experiment 2A were tabulated and the 90% crossover points were calculated and plotted in the summary graph of Fig. 10. Experiment 2B results are shown in Fig. 11.

C. Experiment 3

The corner detection test asked the subject to determine if a synthetic ridge was square (had sharp edges) or round (had a smooth profile). The summary plot, derived from the 90% crossover values, is shown in Fig. 12.

D. Experiment 4

Size discrimination experiments were performed in two groups, one for each shape of ridge. Experiment 4A results (square cross-section ridges) for all test subjects were tabulated and a summary of the results is presented in Fig. 13. Experiment 4B results (round cross-section ridges) are shown in Fig. 14, constructed using the 90% correct crossover points from the data for all subjects.

E. ANOVA Results

To determine the confidence interval for each experiment, three-way analysis of variance (ANOVA) tests were performed for all perception experiments. Results are shown in Table II. Two treatments, the levels of force saturation and the feature sizes or size differences, are used, and results are blocked on

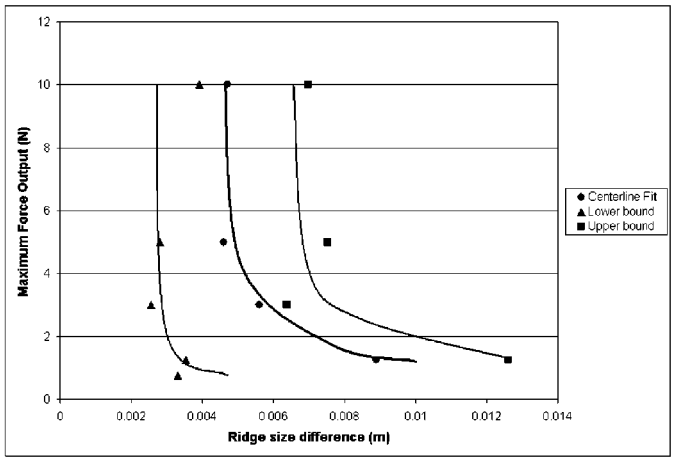

Fig. 14. Experiment 4B (round-ridge size discrimination) summary. Maximum-force output versus ridge size difference for 90% accuracy.

TABLE II
ANOVA CONFIDENCE INTERVALS FOR ALL PERCEPTION EXPERIMENTS

Experiment		Treatment #1 F_{sat} level	Treatment #2 Ridge size or d	Block Subjects	#1-#2 Interaction	#1-Block Interaction	#2-Block Interaction
1A	Square ridge size id	99%	99%	99%	90%	99%	99%
1B	Round ridge size id	99%	99%	99%	6%	99%	77%
2A	Square ridge detection	99%	99%	99%	61%	99%	99%
2B	Round ridge detection	99%	99%	99%	97%	99%	99%
3	Corner detection	99%	99%	99%	99%	99%	92%
4A	Square size discrim	99%	99%	99%	18%	99%	99%
4B	Round size discrim	99%	99%	99%	92%	99%	99%

subjects. Results for all of the experiments indicate that the variations in the data are attributable to the variations in the sizes of objects presented, the force levels, and across subjects with 99% confidence.

For some experiments, there are two-way interactions, most frequently seen when one of the treatments is analyzed for interaction with the variation in subjects. To analyze these interactions, the data were plotted for both the force-subject and size-subject pairs. As expected, one subject with performance trends that did not match the other subjects was the major cause of these interactions. Excluding the data from these contradictory subjects and retabulating the results would give a more detailed analysis and would presumably remove the effects of these interactions.

High confidence intervals also exist for interactions between forces and sizes for the object and corner detection experiments. The most likely reason for this is that the method of simulating surfaces in a haptic environment as a spring and damper implies that force output is proportional to penetration depth in the surface. For the sizes of ridges used in the detection experiments, force output was limited by geometry of the ridges rather than by saturations applied in the computer code. Therefore, the interactions were attributable to the relationship between stimulus size and force output.

F. Force Saturation Data

In order to show actual force output levels that are generated in the simulation, unsaturated and saturated force data were recorded during simulations with both square and round cross-section ridges. Fig. 15 illustrates force versus time data for a typical square-ridge simulation. For this case, forces were saturated at 10 N. For sliding interactions between the stylus and the simulated ridge, output forces are primarily in the range of 5–10 N. When the user taps the stylus on a rigid surface, forces of up to nearly 25 N are generated. For this simulation, the user felt the saturated forces, and both saturated and unsaturated force levels were recorded in a data file. Fig. 16 illustrates force versus time data for a typical interaction with a round ridge. For this case, force levels were saturated at 2 N. Again, the user felt the saturated forces, but both saturated and unsaturated force levels were recorded in a data file. The motion of sliding over the ridge generates forces in the range of 2–8 N, while tapping on the rigid surfaces generates forces of over 10 N.

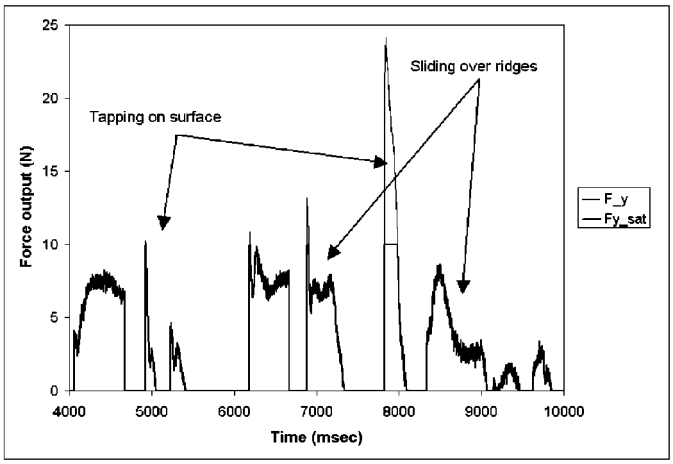

Fig. 15. Y axis force output for user interaction with square ridge, saturating at ± 10 N.

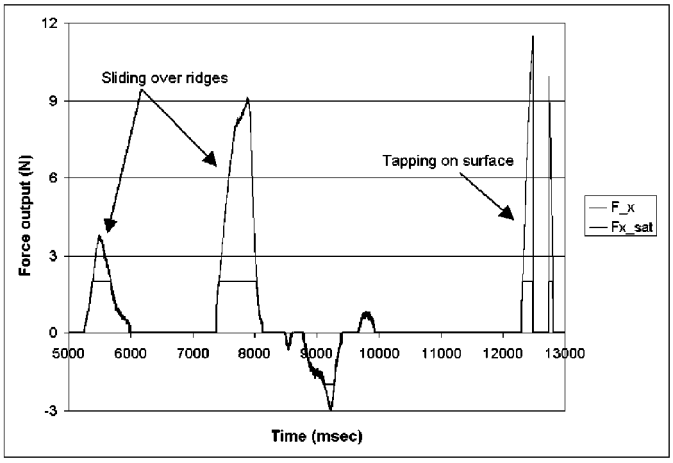

Fig. 16. X axis force output for user interaction with round ridge, saturating at ± 2 N.

IV. DISCUSSION

To best represent the trends for the averages among all test subjects, the authors constructed the trend lines visible in each experiment summary graph. As indicated by the trend lines for the size identification tasks of experiment 1, shown in Fig. 8 and 9, the limit of human perception is approached rather asymptotically, and could be considered as achievable before the max-

imum-force feedback limits of the experimental haptic device were reached. The best average human performance for size identification in this study was reached at maximum-force feedback levels of approximately 3 N for both square and round cross-section ridges. By adding higher levels of force feedback, the designer might be improving the reality of the simulation as compared to touch interactions with nonsynthetic objects, but would not, according to the results presented here, convey significantly more usable information to the human with regard to size identification.

Minimum and maximum performance bounds were also added to the summary graphs in Figs. 8 and 9. These bounds correspond to performance one standard deviation above and one standard deviation below the average. When using these results as a design guideline, one should design based on half of all subjects (centerline fit), 84% of subjects (upper bound), or 16% of subjects (lower bound), depending on the performance objective. These percentages correspond to the $\pm$ standard deviation bands.

Overall, the results for experiments 1A and 1B are quite comparable. The smallest identifiable size difference for experiment 1A for the average subject was approximately 6 mm, while for experiment 1B the smallest identifiable size difference was 7 mm. The shapes of the superimposed trend lines for square and round ridge size identification data are quite similar, implying that the tradeoffs between maximum-force feedback levels and minimum identifiable size differences transcend ridge shapes, at least for those investigated in the experimentation described here.

Figs. 10 and 11 show the results for the experiments 2A and 2B. The results for experiment 2A indicate that performance ceases to improve once the force output has reached about 3 N. This level of force feedback corresponded to a ridge size of just under 0.2 mm. Unlike the results for square-ridge detection, performance for experiment 2B seemed to steadily improve as maximum-force output was increased. The peak performance, at a maximum-force output of 10 N, was the detection of ridges with a radius of 0.15 mm. For experiments 2A and 2B, the minimum boundaries are comprised of only one or two data points. For the force output levels without data points in Figs. 10 and 11, the average percent correct values plus one standard deviation resulted in collections of points above the 90% correct line and, therefore, crossover values were not calculated for those force output levels. It should be noted that there were strong interactions between force and size treatments for the object detection tests, determined by the ANOVA analysis. As mentioned previously, the method of simulating surfaces in a haptic environment as a spring and damper indicates that force output is proportional to penetration depth in the surface. A majority of feature radii values used in the detection experiments were less than 1 mm; therefore, force output was limited by geometry of the ridges rather than by saturations applied in the computer code.

Fig. 12 shows the results of the corner detection tests. For these tests, exponential curve fits to the 0.5 and 0.75 N data did not cross the 90% correct line, so the performance summary centerline fit is asymptotic below the 1.25 N data point. Performance at 1.25, 3.0, and 5.0 N is nearly constant, with 90% correct corner detection of ridges of between 2.0- and 2.5-mm radius. Performance at 10.0 N of force feedback was markedly better, with 90% correct scores achievable for a bump size of 1.5-mm radius. There was no obvious upper limit on performance for the range of forces tested in experiment 3.

Figs. 13 and 14 show results of experiment 4. For experiment 4A, performance increases as maximum-force output increases up to about 3 N of force feedback. Beyond this level, where discrimination sizes of about 5 mm are correctly discriminated 90% of the time, performance gains are not significant. For experiment 4B, performance improved noticeably as force feedback levels were increased up to force levels of approximately 4 N. At this level of force feedback, ridge discrimination sizes of 4.5 mm were correctly discriminated 90% of the time. Beyond this point, increased levels of force feedback do not result in increased performance in terms of the percent correct score.

The previously described discrimination tests were performed relative to a base object size of 2 cm. As is standard in perception measurement, the results obtained can be generalized across scales by using Weber's Law. This law states that there is a constant value k, referred to as the Weber fraction, which indicates the proportion by which a standard stimulus must be varied so that such a change can be detected 50% of the time. This constancy fails to hold for low stimulus values where internal noise is a factor, and for high values, where sensory systems act in a distorted manner [21]. To summarize discrimination test results in terms of Weber fractions and, therefore, generalize across size ranges the size discrimination task results involving stylus-type interaction with square and round cross-section ridges, 50% correct scores were calculated for each force saturation level. For size discrimination tasks involving square ridges, Weber fractions ranged from 0.12 for high-force levels, to 0.2 for low-force levels, noting that smaller Weber fractions indicate better discrimination. For round cross-section ridges, Weber fractions ranged from 0.16 for high-force levels to 0.22 for low-force levels. All Weber fractions are calculated using a standard base width of 2 cm, the size of the smallest stimulus for each test pair. These results can be compared to length discrimination tests performed by Durlach *et al.* [8], where Weber fractions of 0.05 to 0.10, for 10- to 20-mm standard lengths, were recorded. Performance levels during the size discrimination experiments performed with the haptic interface were lower than those found by Durlach, but the decrease in performance would be expected given the differences in experimental conditions. Specifically, the experiments described herein used a stylus to probe the environment rather than direct contact with fingers, were performed on haptic interface hardware rather than with real objects, and were considerably more spatial in nature, compared with those of Durlach.

V. Conclusion

Identification, detection, and discrimination tests were performed to characterize the effect of maximum endpoint force on the haptic perception of detail. For haptic simulation in a stylus-type interface, the following relationships were observed. First, endpoint forces above 3–4 N do not provide any significant improvements in performance (defined at 90% accuracy)

for size discrimination and identification tasks with ridges of square and round cross-sections. Second, endpoint forces above 3–4 N do not appear to provide any significant improvements in performance for object detection tasks; however, ANOVA analysis indicates large interactions between the force and size treatments for these experiments. Third, within the testing range of 0–10 N, there is no apparent upper limit of maximum endpoint force for increased performance gains in the corner detection task.

These observations indicate that haptic interface hardware may be capable of conveying significant perceptual information to the user at fairly low levels of force feedback. While higher levels of force output in a haptic simulation may improve the simulation in terms of perceived realism, the results of these experiments indicate that high levels of force feedback are not required to reach maximum information transfer for most aspects of the haptic display of detail.

ACKNOWLEDGMENT

The authors would like to thank all of the perception test volunteers for their contribution as test subjects and objective critics.

REFERENCES

[1] G. C. Burdea, *Force and Touch Feedback for Virtual Reality*. New York: Wiley, 1996.
[2] M. A. Srinivasan, "Haptic interfaces," in *Virtual Reality: Scientific and Technological Challenges*, N. I. Durlach and A. S. Mavor, Eds. Washington, DC: National Academy Press, 1994, ch. 4.
[3] K. E. MacLean, "Emulation of haptic feedback for manual interfaces," Ph.D. dissertation, MIT, Cambridge, MA, 1996.
[4] G. L. Beauregard, M. A. Srinivasan, and N. I. Durlach, "The manual resolution of viscosity and mass," in *Proc. ASME Dynamic Systems and Control Division*, vol. DSC-57-2, 1995, pp. 657–662.
[5] L. A. Jones, "Matching forces: Constant errors and differential thresholds," *Perception*, vol. 18, no. 5, pp. 681–687, 1989.
[6] K. D. Pang, H. A. Tan, and N. I. Durlach, "Manual discrimination of force using active finger motion," *Perception Psychophys.*, vol. 49, no. 6, pp. 531–540, 1991.
[7] H. Z. Tan, M. A. Srinivasan, B. Eberman, and B. Cheng, "Human factors for the design of force-reflecting haptic interfaces," in *Proc. ASME Dynamic Systems and Control Division*, vol. DSC-55, 1994, pp. 353–359.
[8] N. I. Durlach, L. A. Delhorne, A. Wong, W. Y. Ko, W. M. Rabinowitz, and J. Hollerbach, "Manual discrimination and identification of length by the finger-span method," *Perception Psychophys.*, vol. 46, pp. 29–38, 1989.
[9] R. Ellis, O. Ismaeil, and M. Lipsett, "Design and evaluation of a high-performance prototype planar haptic interface," *Adv. Robot., Mechatron., Haptic Interfaces*, vol. DSC-49, pp. 55–64, 1993.
[10] T. L. Brooks, "Telerobotic response requirements," in *Proc. IEEE Conf. Systems, Man, and Cybernetics*, 1990, pp. 113–120.
[11] C. D. Lee, D. A. Lawrence, and L. Y. Pao, "A high-bandwidth force-controlled haptic interface," in *Proc. ASME Dynamic Systems and Control Division*, vol. DSC-69-2, 2000, pp. 1299–1308.
[12] B. D. Adelstein and M. J. Rosen, "Design and implementation of a force reflecting manipulandum for manual control research," in *Advances in Robotics*, H. Kazerooni, Ed. New York: ASME, 1992, pp. 1–12.
[13] J. E. Colgate and J. M. Brown, "Factors affecting the Z-width of a haptic display," in *Proc. IEEE Int. Conf. Robotics and Automation*, 1994, pp. 3205–3210.
[14] P. A. Millman and J. E. Colgate, "Effects of nonuniform environment damping on haptic perception and performance of aimed movements," in *Proc. ASME Dynamic Systems and Control Division*, vol. DSC-57-2, 1995, pp. 703–711.
[15] L. B. Rosenberg and B. D. Adelstein, "Perceptual decomposition of virtual haptic surfaces," in *Proc. IEEE Symp. Research Frontiers in Virtual Reality*, San Jose, CA, Oct. 1993, pp. 46–53.
[16] H. B. Morgenbesser and M. A. Srinivasan, "Force shading for haptic shape perception," in *Proc. ASME Dynamic Systems and Control Division*, vol. DSC-58, 1996, pp. 407–412.
[17] G. A. Gescheider, *Psychophysics: Method, Theory, and Application*, 2nd ed. Mahwah, NJ: Erlbaum, 1985.
[18] C. M. Perry, "Design of a high performance robot for use in haptic interface and force feedback research," Master's thesis, Dept. Mech. Eng., Vanderbilt Univ., Nashville, TN, 1997.
[19] H. Z. Tan, "Identification of sphere size using the PHANToM: Toward a set of building blocks for rendering haptic environment," in *Proc. ASME Dynamic Systems and Control Division*, vol. DSC-61, 1997, pp. 197–203.
[20] G. A. Miller, "Note on the bias of information estimates," in *Information Theory in Psychology*, H. Quastler, Ed., 1954, pp. 95–100.
[21] S. Coren, L. M. Ward, and J. T. Enns, *Sensation and Perception*. New York: Harcourt Brace, 1999.

Marcia O'Malley (S'00–A'01) received the B.S. degree in mechanical engineering from Purdue University, West Lafayette, IN, in 1996 and the M.S. and Ph.D. degrees in mechanical engineering from Vanderbilt University, Nashville, TN, in 1999 and 2001, respectively.

In 2001, she joined the Mechanical Engineering and Materials Science Department, Rice University, Houston, TX, where she is currently an Assistant Professor. Her current research interests include the development of new techniques for the display of augmented feedback in virtual environments, the implementation and study of haptic feedback in simulated and remote environments, and the design and control of wearable robotic devices for rehabilitation and training.

Michael Goldfarb (S'93–M'95) received the B.S. degree in mechanical engineering from the University of Arizona, Tucson, in 1988 and the S.M. and Ph.D. degrees in mechanical engineering from the Massachusetts Institute of Technology, Cambridge, in 1992 and 1994, respectively.

In 1994 he joined the Department of Mechanical Engineering, Vanderbilt University, Nashville, TN, where he is currently an Associate Professor. His current research interests include the design and control of telemanipulator systems, the design of high-energy-density robotic actuators, and the study of haptic interfaces and simulated mechanical environments.